meat technology
Founder and publisher: Institute of Meat Hygiene and Technology, Belgrade

UDK: 637.5.05
ID: 80253705
https://doi.org/10.18485/meattech.2022.63.2.4

Review paper

A review of hyperspectral imaging in the quality evaluation of meat, fish, poultry and their products

Charan Adithya S.[1*]

A b s t r a c t: Meat and meat products are rich sources of nutrition in the daily diet. Quality and safety assessments of foods, including meats, are essential due to their perishability and vulnerability. The need to analyse food products in real time has stimulated the invention of non-destructive measuring systems. Hyperspectral imaging (HSI) combined with various statistical analysis methods such as multiple linear regression (MLR), least squares-support vector machine (LS-SVM), or partial least squares regression (PLSR), was created as a rapid, non-destructive, non-intrusive and chemical-free process to determine important quality aspects and chemo metrics of foods. The HSI system is used to collect spectral and spatial data. This review discusses the recent developments and application of HSI for detecting quality and safety attributes of tenderness, colour, pH, moisture content, marbling, fat, microbial level and adulteration in meat, fish and poultry meat and products. Overall, HSI technology has tremendous potential to classify different parameters in meat and its products.

Keywords: *hyperspectral imaging, classification, meat, quality assessment, safety detection.*

Introduction

Meat has always played a significant role in human diets all over the world (*Jiang et al.*, 2020a). Humans require meat and meat products in order to acquire some basic vitamins, amino acids, proteins, and other useful components (*Jiang et al.*, 2020b). Pork, beef, lamb, chicken, tuna and other muscle foods are perishable and susceptible to alterations. Microbial growth, colour characteristics, tenderness, marbling, fat content, moisture content (MC) and pH affect certain important quality parameters during the post-mortem storage (*Cheng et al.*, 2017). Furthermore, unscrupulous merchants sell adulterated meat products in which cheaper meat, animal offal, meat unfit for human consumption, and non-meat synthetic chemical materials are added for profiteering purposes. Authenticity testing to detect adulteration in meat and meat products is increasingly vital as trade globalises (*Zhao et al.*, 2019). Consumers and producers equally are concerned about the safety of their meat.

Traditional detection approaches have been introduced, including chromatography, immunological procedures, electrophoretic separation of proteins and techniques focused on DNA, as well as manual sorting. These procedures, on the other hand, are time consuming, damaging, demand complicated laboratory analyses and produce many chemicals, generating toxic waste and polluting the environment (*Zhao et al.*, 2019, *Cheng et al.*, 2017). Hyperspectral imaging (HSI) is a comparatively recent advancement that allows for real-time measurement. This approach incorporates conventional optical imaging and spectroscopy into a single device that at the same time can obtain both spectral and spatial data for an element. On account of its spectral signature, spectroscopy detects or evaluates the analytical signal, and imaging converts the acquired data as distribution maps for spatial visualisation. Following that, HIS can be applied to variety of areas. The meat industry has been paying special attention to HSI techniques. Tenderness, colour, water holding capacity, drip loss, springiness, chewiness, chemical composition, microbial spoilage, authenticity, freshness, and identification of adulteration in meat, fish, and poultry are some of the applications. A variety of studies on HSI for measuring meat quality and safety have been published. However, this review addresses the application of HSI for the assessment of both quality and safety parameters of meat.

Hyperspectral Imaging (HSI) System

HSI has been researched for more than two decades and is one of the most commonly used advanced food investigation methods. HSI's food identification ability has been shown in a number of publications, including for poultry and meat products, fruits

[1]*Kongu Engineering College, Department of Food Technology, Perundurai, Erode-638 060 Tamilnadu, India.*

***Corresponding author:** Charan Adithya S., *charanadithyas.20mft@kongu.edu*

and vegetables, cereals and others (*Ma et al.*, 2019). It is a non-destructive food quality and safety testing platform that uses accelerated inspection. Every pixel in the image produced comprises the spectrum of that particular location, i.e., the light-absorbing and/or scattering properties in the spatial field, which can be used to describe the pixel composition. The entire meat chain uses or will use HSI approaches at different levels (*Achata et al*., 2020).

Components of HSI

The major components of HSI are a camera with a charge-coupled device (CCD)/CMOS detector, objective lens, light source, transporter stage, computer with image acquisition and data processing software, motor and power supply. A regular zoom lens, an extremely specific and sensitive spectrograph and a charge-coupled device or complementary metal-oxide semiconductor camera complete the imaging unit, which is a key component for constructing spatial and spectral knowledge of food specimens. The spectrograph's job is to scatter the captured light into a continuous "electromagnetic spectrum". Most HSI spectrographs include optical instruments like prisms, diffraction gratings and automatically regulated liquid crystal tuneable filters or acousto-optic tuneable filters to accomplish this goal. In HSI systems, the light source is critical because it acts as an optical probe in detecting the chemical components and physical structure of the target foods. In hyperspectral reflectance and transmittance imaging systems, a halogen lamp is frequently used to illuminate the target area with a wider spectral range in the visible-near infrared region (VNIR) region.

Principle and Fundamentals of Hyperspectral Imaging

The HSI approach integrates classical optical spectroscopy and computer vision into a single system that simultaneously generates spectral and spatial information about the specimens being tested. The classical spectroscopic equipment produces a single spectrum I (λ), where an imaging system typically produces an image in two dimensional (2-D) data I. As a result, a 3-D hypercube I , λ) is formed. It could be described as a distinct spatial image I for each wavelength (λ) or as a spectrum I (λ) for each single pixel.

By converting incident photons into electrons, the area is detected using a CCD that can control and quantify the intensity of the light received. The hyperspectral images are acquired and calibrated using a computer control system, which also controls the exposure duration, motor speed, combining mode and wavelength range. Scanning of point, line and region are also terms that describe HIS acquisition techniques. Reflecting, transmitting and interacting properties of the image-sensing models are used to distinguish the light source and the optical detector settings.

Since HIS is described as fast, non-destructive, non-intrusive, environmentally safe and a non-chemical tool, it can be used for effectively evaluating food quality in laboratories and research settings, and it has a lot of promise for replacing conventional analytical techniques in on-line industrial applications. In the hypercube structure, the derived spatial and spectral data must be statistically processed as thousands of spectra (to give the spectral signature) scattered across the calculated region (the spatial signature).

Chemo metric analysis is extremely useful for analysing hypercube data. Chemometrics has the potential to minimise the difficulty in acquiring large data sets, to generate classifying and predicting models and to improve the precision and strength of spectral data analysis models. To limit and correct potential interferences associated with scattering, baseline drift, path-length variance and overlapping bands, spectral pre-treatment methods such as multiplicative scatter correction (MSC), standard normal variate (SNV), smoothing, baseline removal and first as well as second derivatives are used. Regression coefficient analysis (RC), principal component analysis (PCA), successive projections algorithm (SPA), uninformative variable elimination (UVE) and genetic algorithms (GA) are common techniques for selecting the highly educative regions of spectra/optimum wavelengths to simplify the modelling and model construction. Partial least squares regression (PLSR), multiple linear regression (MLR), least squares-support vector machine (LS-SVM) and artificial neural network (ANN) are some of the most commonly used modelling approaches for quantitative analysis. The resulting system is evaluated using numerous statistical parameters that include: calibration (C), cross-validation (CV), and prediction (P) determination coefficients; the corresponding root mean square errors calculated by calibration (RMSEC), cross-validation (RMSECV) or prediction (RMSEP), and; the overall indication factor that is the residual predictive deviation (RPD). In general, a good model should have higher C, CV, P, and RPD values and lower RMSEC, RMSECV, and RMSEP values, while there should be slight discrepancy between them (*Cheng et al.,* 2017).

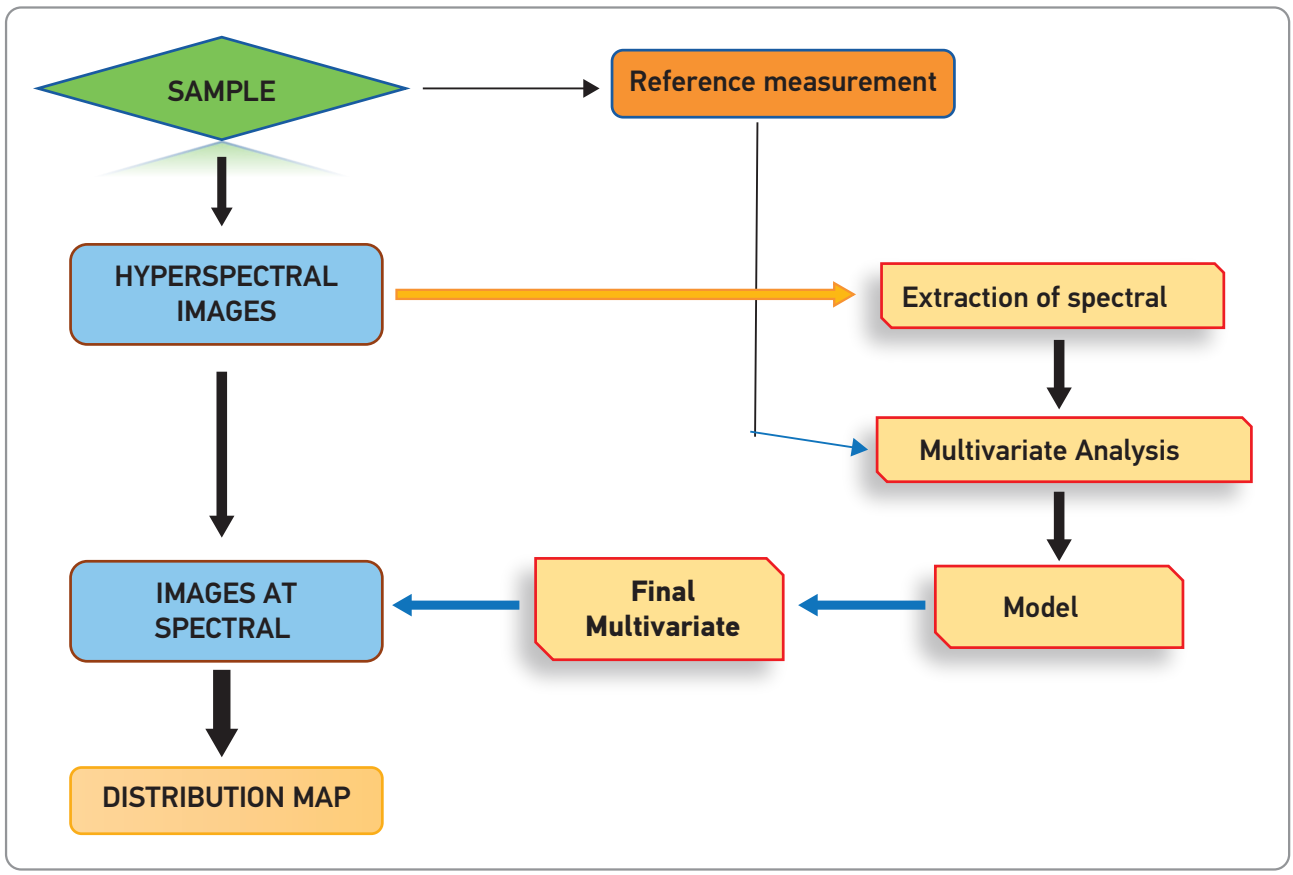

Figure1. Data acquisition using hyperspectral imaging with the multivariate analysis model.

Quality Evaluation

The quality of meat and meat products, which is influenced by their tenderness, colour, pH, MC, fat, marbling, microbial level and adulteration, was evaluated using the HSI systems presented in Table 1. Various statistical methods that were used for detection are also shown in Table 1.

Table 1. Assessment of meat quality and safety traits using hyperspectral imaging

Tested meat specimen	Parameter	Model	Spectral Range (nm)	Accuracy Values	Reference
Beef	Tenderness	HSI-NIR, PLSR	900–1700 nm	cv – 0.83, RMSECV – 40.75 N	(*ElMasry et al.*, 2012)
Fresh Boiler Breast Fillets	Tenderness	HSI - PLS-DA	400–1000 nm	Rp – 0.84	(*Jiang et al.*, 2018)
Beef	Tenderness	VNIR- HSI	400–1000 nm	SSF – 205.8 to 254.8 N Efficiency – 94.40%	(*Naganathan et al.*, 2008)
Beef	Tenderness	HSI - NIR, MLR	900–1700 nm	R – 0.89	(*Saadatian et al.*, 2015)
Beef	Tenderness	HSI - WBS	496–1036 nm	R – 0.67	(*Cluff et al.*, 2008)
Hanging Beef Carcasses	Tenderness	HSI	400–1000 nm	SSF – 18.9% TO 81.1%, Efficiency – 87.60%	(*Naganathan et al.*, 2015)
Salmon Fillets (Raw Farmed)	Tenderness	VNIR - HSI, PLSR & LS-SVM	400–1720 nm	Rp – 0.949, RMSEP – 1.089, RPD – 2.339	(*He et al.*, 2014)

Tested meat specimen	Parameter	Model	Spectral Range (nm)	Accuracy Values	Reference
Chicken breast fillets	Colour (L*)	HSI, PLSR	400–1000 nm	L* - Rp − 0.85, RMSEP − 40.75 N	(*Yang et al*., 2021)
Salmon Fillet	Colour (L*a*b*)	LW-NIR - HSI	900–1700 nm @ 256 bands	L* => Rp − 0.864 RMSEP − 2.424 a* => Rp − 0.736 RMSEP − 1.454 b*=>Rp − 0.798 RMSEP − 2.060	(*Wu et al*., 2012)
Beef, Lamb, Pork	Colour (L*a*b*)	HSI - MLR	400–1000 nm	L* => p − 0.94 RMSEP − 1.89 a* => p − 0.91 RMSEP − 1.40 b* => p − 0.83 RMSEP − 1.37	*(Kamruzzaman et al*., 2016)
Beef	Colour (L*a*b*)	HSI-NIR, PLSR	900–1700 nm	L* => cv – 0.88 RMSECV – 1.21 a* => *not satisfactory b * => cv – 0.81 RMSCV – 0.58	(*ElMasry et al*., 2012)
Beef	Colour (L*a*b*)	HSI, SG-RC-MLR	400–1000 nm	L* => p – 0.858 RMSEP – 0.808 a* => p – 0.890 RMSEP – 0.735 b* => p – 0.8161 RMSEP – 0.521	(*Liu et al*., 2018)
Turkey Ham	Colour (L*a*b*)	HSI-NIR, PLSR	900–1700 nm	L* => cv – 0.18 RMSECV – 1.66 a* => cv – 0.74 RMSECV – 0.35 b* => cv – 0.49 RMSECV – 0.89	(*Iqbal et al*., 2013)
Chicken breast fillets	pH	HSI-VNIR, PLSR	400–1000 nm @473 bands	Rp – 0.854 RMSEP – 0.13	(*Yang et al*., 2021)
Beef	pH	HSI-NIR, PLSR	900–1700 nm	cv – 0.73 RMSEP – 0.06	(*ElMasry et al*., 2012)
Chicken	pH	HSI-VNIR, PLSR	400–1000 nm	– 0.80 to 0.84 RMSE – 0.16 to 0.18	(*Kaswati et al*., 2020)
Beef	pH	HSI - SVM	400–1000 nm	99% accuracy pH – 5.8	(*Crichton et al*., 2017)
Salted Pork	pH	HSI, PLSR	400–1000 nm	p – 0.794 RMSEP – 0.086	(*Liu et al*., 2014)
Turkey Ham	pH	NIR - HSI, PLSR	900–1700 nm	cv – 0.81 RMSECV – 0.02	(*Iqbal et al*., 2013)
Beef	Moisture Content	HSI, SG-SPA-LS-SVM	400–1000 nm	p – 0.869 RMSEP – 1.304	(*Liu et al*., 2018)
Ground Beef	Moisture Content	NIR-HSI, PLS	880–1720 nm	p – 0.82 RMSEP – 1.77% (w/w)	(*Zhao et al*., 2017)
Lamb meat	Moisture Content	NIR-HSI, PLSR	900 –1700 nm	p – 0.88 RPD – 2.63	(*Kamruzzaman et al*., 2012)

Tested meat specimen	Parameter	Model	Spectral Range (nm)	Accuracy Values	Reference
Turkey Ham	Moisture Content	NIR-HSI, PLSR	900 –1700 nm	cv – 0.88 RMSECV – 2.51	*(Iqbal et al.*, 2013)
Pork	Moisture Content	HSI, PLSR	400–1000 nm	p – 0.94 RMSEP – 0.7682	(*Ma et al.*, 2017)
Cooked Beef	Moisture Content	HSI, BP-ANN, PLSR	400–1000 nm @ 774 bands	p – 0.977 RMSEP – 0.915	(*Yang et al.*, 2017)
Salmon Fish	Moisture Content	HSI, PLSR & LS-SVM	400–1753 nm	Rp – 0.815 to 0.970 RMSEP – 0.312% to 1.147%	(*Wu and Sun,* 2013a)
Beef	Microbial Growth - TVC	VNIR- HSI, PLSR	957–1664 nm	p – 0.86 RMSEP – 0.89 log CFU/g	(*Achata et al.*, 2020)
Chicken	Microbial Growth - *Pseudomonas spp. & Enterobacteriaceae*	NIR- HSI, MSC-PLS	900–1700 nm	Rp – 0.954 RMSEP – 0.396 log10 CFU/g	(*Jiang et al.*, 2021)
Spiced Beef	Microbial Growth - Total Viable Count	HSI, N-PLS	400–1000 nm @ 774bands	p – 0.934 RMSEP – 0.755	(*Yang et al.*, 2018)
Pork Meat	Microbial Growth - Total Viable Count	HSI	430–960 nm	p – 0.8308 RMSECV – 0.243 log CFU/g	(*Huang et al.*, 2013)
Chicken Meat Surface	Bacterial Contamination - Total Viable Count	HSI - TBFI	400–1000 nm	– 0.6833	(Ye et al., 2016)
Grass Carp Fish Flesh	Microbial Growth - *E. coli*	HSI - PLSR & MLR	400–1000 nm	p – 0.870 RMSEP – 0.274 log CFU/g	(*Cheng and Sun,* 2015)
Porcine meat (pork)	Microbial Growth - TVC, PPC	HSI - NIR	900–1700 nm @ 256 bands	– 0.82 to 0.85	(*Barbin et al.*, 2013)
Salmon Flesh	Microbial Growth - Total Viable Count	TS-HSI-VNIR, PLSR	400–1700 nm	p – 0.985 RMSEP – 0.280	(*Wu and Sun*, 2013b)
Pork Meat	Microbial Growth - *E. coli*	HSI - Gompertz function	400–1100 nm	Rcv – 0.939 RMSECV – 0.6369	(*Tao and Peng*, 2014)
Beef & Chicken	Adulteration of beef with chicken	HSI, GD-RC	380–1000 nm, with 950bands	Rp – 0.9831 RMSEP – 0.0319	(*Zhao et al.,* 2020)
Beef	Adulteration of beef with spoiled beef	VNIR - HSI, methods - PLSR, SVM	496–1000 nm, 250 bands	p – 0.95 RMSEP – 5.67%	(*Zhao et al.*, 2019)
Beef	Adulteration of beef with duck meat	VNIR - HSI, methods - PLSR, PCR	400–1000 nm	p – 0.96 RMSEP – 6.58%	(*Jiang et al.*, 2019)
Beef & Pork	Adulteration of plant and animal based in beef & pork	HSI, PLSR	400–1000 nm	R – 0.69 RPD – 1.41 to 2.82	(*Rady and Adedeji,* 2020)

Tested meat specimen	Parameter	Model	Spectral Range (nm)	Accuracy Values	Reference
Chicken	Adulteration of chicken with carrageenan	VNIR - HSI, PLSR	400–1000 nm	p – 0.85 RMSEP – 0.93	(*Zhang et al.,* 2019)
Pork Minced	Adulteration of minced pork with minced pork jowl meat	HSI, RC-PLSR	400–1000 nm	p – 0.9063 RMSEP – 13.93%	(*Jiang et al.,* 2020a)
Minced Beef	Adulteration of minced beef with pork & duck meat	NIR - HSI, DA / PLS	980–1800 nm	Rp – 91.62 to 95.8% RMSEP – 9.27 to 10.3	(*Leng et al*., 2020)
Lamb, Beef, Pork	Adulteration of red meat	HSI, SVM/CNN	548–1701 nm	94.40% accuracy	(*Al-Sarayreh et al.*, 2018)
Prawn	Adulteration of prawn with gelatin	HSI, LS-SVM	441–1030 nm	p – 0.962 RMSEP – 0.339	(*Wu et al*., 2013)
Minced Beef	Adulteration level of minced beef with horse meat	VNIR - HSI, PLSR	400–1000 nm	p – 0.98 RMSEP – 2.20%	(*Kamruzzman et al.* 2015)
Pork Minced	Adulteration pork minced with fats of leaf lard	HSI, PLSR	400–1000 nm	p – 0.98 RMSEP – 4.87%	(*Jiang et al.,* 2020b)
Beef	Marbling	HSI - PLSR	400–1000 nm	Rp – 0.95 RMSEP – 0.3BMS	(*Aredo et al*., 2017)
Pork	Marbling	HSI - NIR	900–1700 nm	Rp – 0.90 RMSEP – 0.52	(*Huang et al*., 2014)
Pork	Marbling	HSI	430–1000 nm	3.0 to 5.0 %	(*Qiao et al.*, 2007)
Beef	Marbling	HSI	400–1100 nm	cv – 0.92 RMSEP – 0.45	(*Li et al*., 2011)
Beef	Marbling	HSI	400–1000 nm	– 0.91	(*Lohumi et al.*, 2016)
Beef	Marbling	HSI	400–1000 nm	Error – 0.08% Level of prediction – 0.99%	(*Velásquez et al.*, 2017)
Ground Beef	Fat	NIR-HSI, PLS	880–1720 nm	p – 0.90 RMSEP – 1.72 to 1.83% (w/w)	(*Zhao et al.*, 2017)
Lamb meat	Fat	NIR-HSI, PLSR	900–1700 nm	p – 0.88 RPD – 3.20	(*Kamruzzaman et al.*, 2012)
Pork	Fat	HSI - PLSR	900–1700 nm	– C14:0 to C18:2 RMSECV – 0.087 to 0.304 mg/g	(*Kucha et al*., 2020)
Pork	Fat	NIR-HSI	900–1700 nm	Rp – 0.83	(*Huang et al*., 2017)
Salmon fillets	Fat	NIR-HSI, LV-SVM	900–1700 nm	Rp – 0.9685 RMSEP – 1.1750	(*Zhang et al*., 2020)
Lamb	Fat	HSI	954–1677 nm	– 0.59 RMSE – 2.34 mm	(*Rahman et al*., 2018)

Tenderness

Tenderness is an essential trait of meat consistency, characterised by chewing ease. It has been commonly used as a consumer-perceived proxy for the eating consistency of beef (*Jiang et al.,* 2018). Consumer approval of meat is based on tenderness, so it is vital for the meat industry to deliver high-quality, safe-to-eat, tender meat (*Saadatian et al.*, 2015). Flaws in meat quality, particularly in tenderness, have resulted in lower consumer loyalty and, as a result, lower market share. According to recent reports, about 15–20% of meats offered to consumers are not tender (*Cluff et al.*, 2008). In the meat industry, meat tenderness is currently determined mostly by the use of shear force equipment or sensory evaluation. These techniques, on the other hand, are time-consuming, destructive, and incompatible with the rapid-paced manufacturing and processing environments used in meat plants (*Tao and Peng*, 2014). *Cluff et al*. (2008) combined HSI with Warner-Bratzler shear force (WBSF) to collect tenderness reference values. The established model predicted WBSF scores (R = 0.67). However, the applied model showed limitations in predicting tenderness in beef. *ElMasry et al*. (2012) combined HSI operating in near the infrared region (NIR) with a PLSR model, which resulted in good prediction in the 900–1700 nm range (c – 0.91, RMSEC – 29.42 N, cv – 0.83, RMSECV – 40.75 N). More research is required to improve the model's prediction, accuracy and reliability. *He et al*. (2014) demonstrated tenderness evaluation in fresh farmed salmon fillet with HSI operating in VNIR at 400–1700 nm combined with PLSR and LS-SVM models, which resulted in the strongest performance among the systems examined (Rp – 0.905, RMSEP – 1.089, RPD – 2.339). The results indicated that combining HSI with LS-SVM showed better performance for predicting tenderness in salmon fillets. *Jiang et al*. (2018) used HSI combined with a PLS-DA model in the spectral range 400–100 nm for fresh chicken, and showed the model strongly predicted tenderness (Rp – 0.84, RC – 0.94). Similarly, pork meat tenderness analysed using HSI combined with MLR model showed reasonably good prediction (Rcv – 0.949, RC – 0.995, SEC – 2.796, SECV – 5.702).

Colour

In the meat industry and meat science study, colour is a significant element that is widely seen as a quality index. Consumers identify colour loss mainly as an indicator of lack of freshness and wholesomeness, so colour has been identified as a crucial meat quality attribute that affects the purchasing decision (*Kamruzzaman et al.*, 2016). Meat colour is also affected by the amount of protein pigments and myoglobin in the muscle. The quality and proportion of bound myoglobin establishes lightness (L*), redness/greenness (a*) and yellowness/blueness (b*) values (*Liu et al*., 2018). L* values are used to categorise pork into three groups, i.e. dark, firm, and dry (DFD), normal (NORM), and pale, soft, and exudative (PSE) (*Yang et al*., 2021). Conventional methods, such as using a colorimeter to assess lightness (L*), a* and b*, usually involve interaction with meat surfaces, which could contribute to contamination (*Liu et al*., 2018). As a result, developing a fast and non-destructive system for assessing meat quality is of great importance. *Kamruzzaman et al*. (2016) examined a HSI system at 400–1000 nm with the MLR model for red meat colour; the prediction results were: L* – (p – 0.94, RMESP – 1.89, RPD – 4.12); a* – (p – 0.91, RMSEP – 1.40, RPD – 3.79) and; b* – (p – 0.833, RMSEP – 1.37, RPD – 2.29), which proved good performance for predicting the red meat colour. A HSI system operating in the NIR region at 901–1710 nm combined with a PLSR model was used to determine the colour information of meat (*ElMasry et al*., 2012). The model showed good predicting results for L*– (cv – 0.88, RMSEP – 1.21) and b* – (cv – 0.81, RMSEP – 0.58). However, a* values were not satisfactory because the fell in a narrow range.

pH

pH is one of the most important consistency characteristics of beef. After being slaughtered, the acidity of meat increases (*Kaswati et al.*, 2020). pH is an important technical factor that influences microbial development. It also has a major effect on meat colour, flavour, water holding capacity, water activity and shelf life. During salting, protein precipitation and solubilisation cause the pH of meat products to change. In salted and dry cured beef, pH is linked to water holding capacity and loss of water. pH can also differentiate pork into three categories, i.e. DFD, NORM and PSE (*Yang et al*., 2021). A portable pH meter or a surface electrode are widely used to measure pH, but they are destructive and unstable methods, unsuitable for large-scale industrial applications. A HSI that operated in the VNIR region at 400–1000 nm was used to determine the pH of chicken meat. A fully cross-validated PLSR model was used (*Yang et al.,* 2021), and measures (Rp – 0.854, RMSEP – 0.13) showed the

resulting model had good prediction rates. A similar model (VNIR-HSI, PLSR) was used (*Kaswati et al.*, 2020) for pH prediction in chicken meat. The system yielded close results on fresh (– 0.80, RMSE – 0.16) and spoiled (– 0.84, RMSE – 0.18) chicken. Another HSI system in the NIR region, at 900–1700 nm in combination with PLSR model resulted in strong prediction of pH in beef compared to other models (c – 0.83, RMSEC – 0.05, cv – 0.73, RMSECV – 0.16) (*ElMasry et al*., 2012). Parallel results were obtained with HSI system in the NIR region in combination with a PLSR model for turkey and ham at 900–1700 nm (c – 0.88, RMSEC – 0.02, cv – 0.81, RMSECV – 0.02) (*Iqbal et al*., 2013). The overall pH present in the meat and meat products was predicted to be from pH 5.3 to 6.2.

Moisture Content (MC)

Since water is a vital element of meat and meat products, MC is one of the most essential properties that determines the quality and safety of meats. Changes in MC have a significant impact on microbial growth and meat quality traits (such as flavour, juiciness and appearance), processed meat storage time and consumer purchasing desires. MC is usually measured using a number of conventional techniques, including drying using a hot air oven, microwave drying, freeze drying and infrared moisture analysis (*Yang et al.*, 2017). However, because of their time-consuming and complicated processes, general moisture analysis approaches are not suitable for evaluating a large number of samples. HSI technique was used to determine the MC in cooled meat samples (*Liu et al.*, 2018) at 400–1000 nm using a SPA-LS-SVM model, but results were not encouraging (p – 0.869, RMSEP – 1.304, RPD – 2.724). However, better results were obtained in another study using HSI in combination with BP-ANN and PLSR to model cooked meat at 400–1000 nm (p – 0.977, RMSEP – 0.915) (*Yang et al.*, 2017). These results were superior to those of other prediction models. Moisture content in salmon fish was better predicted by combining HSI with PLSR and LS-SVM models at 400–1753 nm (p – 0.872 to 0.934, RMSEP – 0.312% to 1.147%, RPD – 1.082 to 4.034) (*Wu and Sun*, 2013a). Similarly, MC in other red meats (pork, lamb) was detected using HSI in NIR region at 400–1700 nm with a PLSR model (p – 0.88, 0.942, RMSEP – 0.7682, 1.4736) (*Kamruzzaman et al.*, 2012, *Ma et al.*, 2017). The overall prediction of MC in meat and meat products showed good results using HSI system.

Microbial Level

During storage, the wet, nutrient-rich fresh meat surface facilitates the growth of wide variety of spoilage bacteria. As a result, the total viable count (TVC) of bacteria is a valuable indicatior of meat's microbial control. When the TVC in meat exceeds a certain level, the bacteria tend to be pathogenic. However, since meat has adequate moisture and nutrients required for microbial growth and reproduction, particularly for the dominant spoilage microorganisms, chilled meat can harbour and support growth of *Pseudomonas* and *Enterobacteriaceae* at 0–4°C (*Jiang et al.*, 2021). Cross contamination of meat carcasses with *Escherichia coli*, *Salmonella* and other bacteria can occur during the processing steps like bleeding, scalding, feather removal, cleaning, chilling, and secondary processing (*Cheng and Sun*, 2015). To predict bacterial spoilage in meat, numerous chemical, physical and microbiological techniques were suggested. The majority of these techniques, on the other hand, take a lot of time, are destructive, involve complicated laboratory processes and require repetitive sample preparation. As a result, the HSI approach to rapidly and precisely diagnose microbial spoilage in meat is widely used. *Achata et al*. (2020) studied TVC in beef using HSI in the VNIR region at 957–1664 nm using PLSR model. The results were not ideal (p – 0.86, RMSEP – 0.89 log CFU/g, RPD – 2.27). Using the same system (*Yang et al*., 2018) but with different modelling strategies, N-PLS at 400–1000 nm, yielded better prediction results (p – 0.934, RMSEP – 0.755) for TVC in beef. Similarly, *Wu and Sun* (2013b) predicted TVC in salmon fish, using HSI in the VNIR region at 400–1700 nm with PLSR modelling technique, and showed this system had better performance (p – 0.985, RMSEP – 0.280, RPD – 5.127). *Cheng and Sun* (2015) used the same HIS system to predict whether there was *E. coli* contamination in fish using the PLSR and MLR technique at 400–1000 nm, (p – 0.870, RMSEP – 0.274 log CFU/g, RPD – 5.22). Similarly, *Jiang et al.* (2021) investigated the growth of *Pseudomonas* and *Enterobacteriaceae* in chicken under cold storage with HSI system operating in the NIR region at 9000–1700 nm in combination with MSC-PLS model, and achieved good prediction results (p – 0.954, RMSEP – 0.396 log CFU/g, RPD – 3.33).

Adulteration

Adulteration and authenticity identification in meat and their products is becoming highly relevant as trade globalises (*Zhao et al.*, 2019). Meat adulteration has direct impacts on consumer interests and can pose

many health risks. The horsemeat scandal in Europe several years back, for example, exposing meat adulteration process around the world, resulted in a major public confidence calamity (*Leng et al.*, 2020). Meat composition products, such as hamburgers, meatballs, patties, salami and sausages, often use minced or finely chopped meat as a key component. Partial or complete substitution of cheaper meat or addition of proteins from animal or vegetable origins to minced meat and similar ingredients can be tempting to dishonest meat chain actors. Compared with several other spectroscopic studies for detecting adulteration in meat and meat products, HSI was the best rapid, non-destructive analytical technique to detect the level of adulteration. *Kamruzzman et al*. (2015) determined the adulteration level of minced beef adulterated with horse meat using HSI in the VNIR region at 400–1000 nm with a PLSR model, which, among the systems examined, yielded the best performance in prediction rates (p – 0.98, RMSEP – 2.20%). Using the same system with the GD-RC model at 380–1000 nm predicted beef adulterated with chicken meat (R – 0.9831, RMSEP – 0.0319) (*Zhao et al.*, 2020). *Jiang et al*. (2020a) and *Jiang et al.* (2020b) experimented to detect the adulteration of minced pork with two different adulterants, namely minced pork jowl meat and leaf lard fats. A HSI system with PLSR modelling strategy was established at 400–1000 nm which showed prediction results for minced pork jowl meat adulterant (p – 0.9063, RMSEP – 13.93%, RPD – 2.30, LOD – 6.50%) and leaf lard adulterant (p – 0.98, RMSEP – 4.87%, RPD – 6.57, LOD – 6.08%). In addition, HSI was considered for the detection of adulteration in prawns after the animals ingested gelatine that had been extracted from mammal animal skins and bones using LS-SVM model at 441–1734 nm range (*Wu et al.*, 2013). The resultant prediction indicators were p – 0.962, RMSEP – 0.339, RPD – 5.128.

Marbling

Marbling is characterised by the volume and spatial distribution of visible fat that occurs as thin layers in the muscle, whereby the entire tissue resembles marble. It is considered to be a major meat trait that affects the acceptability of meat and their products. Fat lines that are evenly spread around the surface of the beef cause marbling that is commonly associated with higher meat quality. The quantitative and spatial distribution of fat lines in meat and meat products that contain pork and beef, in which marbling defines and distinguishes the commodity, lead to variations in eating consistency (*Velásquez et al.*, 2017). Marbling is a critical criterion for determining the consistency of beef. It is linked to the tenderness and flavour of beef. In general, beef with a lot of marbling has a tender feel (*Li et al.*, 2011). Marbling detection is labour-intensive and difficult to visually grade, which makes it hard for a human observer to correctly determine the scores for marbling. Because of such drawbacks, the traditional approach is not suited for a fast-paced on-line operation (*Huang et al.*, 2014). A HSI system that operated in the NIR region was established to detect marbling in meat products. *Aredo et al.* (2017) combined the HSI system with a PLSR model at 400–1000 nm to measure marbling in beef; the system proved to be the most efficient method among those examined and resulted in Rp – 0.95, RMSEP – 0.3 BMS, Rc – 0.98, RMESC – 0.2 BMS. Another study using the same system by *Huang et al*. (2014) showed the marbling in pork meat at 900–1700 nm spectral range with results of Rv – 0.90, RMSEV – 0.52, Rc – 0.91, RMSEC – 0.34. This established the good performance of the HIS system in detecting the level of pork meat marbling.

Fat

Intramuscular fat (IMF) content in meat is described as the total amount of dispersed spots of fat within edible muscle. It reflects the amount of fat in meat, and has a considerable effect on meat cooking quality, consumer satisfaction and consumer health. Although higher IMF levels are associated with greater market acceptance, consumer preferences differ by geographic location (*Huang et al.*, 2017). The content and structure of the IMF have a significant impact on other consistency attributes including juiciness, tenderness and flavour. The IMF is released during mastication that activates the salivary glands, resulting in juiciness. Fat improves muscle tenderness by weakening the muscle's elastic strength and preventing cross-linking between connective tissue and muscle fibre proteins, allowing the muscle to be split open easily in the mouth with less friction. Because of their contact with Maillard reaction products to liberate volatile compounds during the cooking of beef, fatty acids affect meat taste *(Kucha et al.*, 2020). *Zhao et al.* (2017) studied fat content in beef using a HSI system in the NIR region 880–1720 nm with PLSR, and computed the following results: p – 0.90, RMSEP – 1.72% to 1.83% w/w. Another study was carried out using the same system (*Kamruzzaman et al.*, 2012) for determining the fat content in lamb meat at spectral range 900–1700 nm gave the prediction statistics

of p – 0.88, RMSEP – 0.35%, RPD – 3.20. The results indicated HIS would be much better for detecting fat percentage in lamb meat than the other chemometric analysis methods. Similarly, other studies were conducted for pork (*Huang et al.*, 2017) and fish (*Zhang et al.*, 2020) in the spectral range 900–1700 nm showed reasonably good prediction statistics of Rp – 0.83 for pork and Rp – 0.9685 for fish.

Future Trends and Challenges

Despite the above benefits, HSI has several restrictions in meat industry applications. One such concern is the speed of HSI, which is a major downside. It requires a very long time for handling, displaying and processing the data. As a result, the HSI systems' speeds must be increased in order to speed up the collection and examination of spectral data. The cost of HIS is another drawback to its widespread application. HSI systems are considerably more expensive than multispectral imaging systems. For the outcome in real time applications, a multispectral imaging device of chosen wavelengths is an alternate promising solution. HIS has been researched by several groups in order to determine the most powerful wavelengths for constructing on-line multispectral imaging instruments. Since HSI is used to develop dedicated multispectral vision systems, it is important to think about wavelength range in all HIS techniques. The agricultural industry would benefit greatly if the food processing industry could incorporate spectral imaging technologies in real-time modes. However, a major significant drawback of HSI is that it is not a direct tool, and so its implementation involves systematic calibration and model transition procedures. As a result, moving these off-line lab applications to an on-line manufacturing environment will take more time and resources.

Conclusion

The quality and safety evaluation of meat and meat products that is achieved by rapid, objective, and non-destructive calculation and prediction of technical parameters and various classifications is crucial. HIS incorporates the complete benefits of spectroscopy and computer vision, which are the two traditional techniques used. HIS systems offer both spatial and spectral information; as a result, this technology provides new sensing capabilities that improve beef, poultry, and fish examination. In this review, the application of HSI to detect quality and safety attributes of tenderness, colour, pH, moisture content, microbial level, adulteration level, marbling and fat percentage in meat and meat products was presented. Various chemometric parameters can be predicted with HIS systems in different spectral ranges and predicted results are then analysed statistically (by tools like PLSR, MLR, LS-SVM). The results show that spectral data could be used to replace laborious and time-consuming standard analytical methods, offering a simple and non-destructive testing tool for the meat industry. However, there is still potential for progress in the production of low-cost multispectral imaging systems for particular applications. The important wavelengths specified in this review can be used to build HIS systems for specific applications.

Hiperspektralno snimanje u proceni kvaliteta mesa, ribe, živine i njihovih proizvoda

Charan Adithya S.

A p s t r a k t: Meso i proizvodi od mesa su bogati izvori hranljivih sastojaka u svakodnevnoj ishrani. Procena kvaliteta i bezbednosti hrane, uključujući mesa, su od suštinskog značaja zbog njihove kvarljivosti i osetljivosti. Potreba za analizom prehrambenih proizvoda u realnom vremenu podstakla je pronalazak nedestruktivnih mernih sistema. Hiperspektralno snimanje (HSI), u kombinaciji sa različitim metodama statističke analize, kao što su višestruka linearna regresija (MLR — Multiple Linear Regression), metoda potpornih vektora koja koristi tehniku najmanjih kvadrata (LS-SVM — Least Squares-Support Vector Machine) ili delimična regresija najmanjih kvadrata (PLSR — Partial Least Squares Regression), kreirano je kao brzi, nedestruktivni, neintruzivni proces bez hemikalija za određivanje važnih aspekata kvaliteta i hemometrike hrane. HSI sistem se koristi za prikupljanje spektralnih i prostornih podataka. Ovaj revijalni rad daje uvid u nedavni razvoj i primenu HSI sistema za otkrivanje kvalitetnih i bezbednosnih odlika kao što su mekoća, boja, pH, sadržaj vlage, mramoriranost, masnoća, sadržaj mikroba i falsifikovanja mesa, ribe i živinskog mesa i njihovih proizvoda. Sve u svemu, HSI tehnologija ima ogroman potencijal da klasifikuje različite parametre mesa i njegovih proizvoda.

Ključne reči: *hiperspektralno snimanje, klasifikacija, meso, procena kvaliteta, detekcija bezbednosti.*

Disclosure statement: No potential conflict of interest was reported by authors.

References

Achata, E. M., Oliveira, M., Esquerre, C. A., Tiwari, B. K. & O'donnell, C. P. 2020. Visible and NIR hyperspectral imaging and chemometrics for prediction of microbial quality of beef Longissimus dorsi muscle under simulated normal and abuse storage conditions. *LWT — Food Science and Technology,* 128, doi.109463.

Al-sarayreh, M. M., Reis, M., Qi yan, W. & Klette, R. 2018. Detection of red-meat adulteration by deep spectral–spatial features in hyperspectral images. *Journal of Imaging,* 4, 63.

Aredo, V., Velásquez, L. & Siche, R. 2017. Prediction of beef marbling using Hyperspectral Imaging (HSI) and Partial Least Squares Regression (PLSR). *Scientia Agropecuaria,* 8**,** 169–174.

Barbin, D. F., Elmasry, G., Sun, D.W., Allen, P. & Morsy, N. 2013. Non-destructive assessment of microbial contamination in porcine meat using NIR hyperspectral imaging. *Innovative Food Science & Emerging Technologies,* 17, 180–191.

Cheng, J. H., Nicolai, B. & Sun, D. W. 2017. Hyperspectral imaging with multivariate analysis for technological parameters prediction and classification of muscle foods: A review. *Meat science,* 123, 182–191.

Cheng, J. H. & Sun, D. W. 2015. Rapid quantification analysis and visualization of Escherichia coli loads in grass carp fish flesh by hyperspectral imaging method. *Food and Bioprocess Technology,* 8, 951–959.

Cluff, K., Naganathan, G. K., Subbiah, J., Lu, R., Calkins, C. R. & Samal, A. 2008. Optical scattering in beef steak to predict tenderness using hyperspectral imaging in the VIS-NIR region. *Sensing and Instrumentation for Food Quality and Safety,* 2, 189–196.

Crichton, S. O., Kirchner, S. M., Porley, V., Retz, ., Von Gersdorff, G., Hensel, O. & Sturm, B. 2017. High pH thresholding of beef with VNIR hyperspectral imaging. *Meat science,* 134, 14–17.

Elmasry, G., Sun, D. W. & Allen, P. 2012. Near-infrared hyperspectral imaging for predicting colour, pH and tenderness of fresh beef. *Journal of Food Engineering,* 110, 127–140.

He, H. J., Wu, D. & Sun, D. W. 2014. Potential of hyperspectral imaging combined with chemometric analysis for assessing and visualising tenderness distribution in raw farmed salmon fillets. *Journal of Food Engineering,* 126, 156–164.

Huang, H., Liu, L. & Ngadi, M. O. 2017. Assessment of intramuscular fat content of pork using NIR hyperspectral images of rib end. *Journal of Food Engineering,* 193, 29–41.

Huang, H., Liu, L., Ngadi, M. O., Gariépy, C. & Prasher, S. O. 2014. Near-Infrared spectral image analysis of pork marbling based on Gabor filter and wide line detector techniques. *Applied Spectroscopy,* 68, 332–339.

Huang, L., Zhao, J., Chen, Q. & Zhang, Y. 2013. Rapid detection of total viable count (TVC) in pork meat by hyperspectral imaging. *Food Research International,* 54, 821–828.

Iqbal, A., Sun, D. W. & Allen, P. 2013. Prediction of moisture, color and pH in cooked, pre-sliced turkey hams by NIR hyperspectral imaging system. *Journal of Food Engineering,* 117, 42–51.

Jiang, H., Cheng, F. & Shi, M. 2020a. Rapid identification and visualization of jowl meat adulteration in pork using hyperspectral imaging. *Foods,* 9, 154.

Jiang, H., Jiang, X., Ru, Y., Wang, J., Xu, L. & Zhou, H. 2020b. Application of hyperspectral imaging for detecting and visualizing leaf lard adulteration in minced pork. *Infrared Physics & Technology,* 110, 103467.

Jiang, H., Wang, W., Zhuang, H., Yoon, S. C., Yang, Y. & Zhao, X. 2019. Hyperspectral imaging for a rapid detection and visualization of duck meat adulteration in beef. *Food Analytical Methods,* 12, 2205–2215.

Jiang, H., Yoon, S. C., Zhuang, H., Wang, W., Lawrence, K. C. & Yang, Y. 2018. Tenderness classification of fresh broiler breast fillets using visible and near-infrared hyperspectral imaging. *Meat Science,* 139, 82–90.

Jiang, S., He, H., Ma, H., Chen, F., Xu, B., Liu, H., Zhu, M., Kang, Z. & Zhao, S. 2021. Quick assessment of chicken spoilage based on hyperspectral NIR spectra combined with partial least squares regression. *International Journal of Agricultural and Biological Engineering,* 14, 243–250.

Kamruzzaman, M., Elmasry, G., Sun, D. W. & Allen, P. 2012. Non-destructive prediction and visualization of chemical composition in lamb meat using NIR hyperspectral imaging and multivariate regression. *Innovative Food Science & Emerging Technologies,* 16, 218–226.

Kamruzzman, M., Yoshio, M., Seiichi, O., Shu, L. (2015). Assesment of visible near infrared -Infrared Hyperspectral Imaging as a Tool for Detection of Horsemeat Adulteration in Minced Beef. *Food and Bioprocess Technologies*, DOI: 10.1007/s11947–015–1470–7.

Kamruzzaman, M., Makino, Y. & Oshita, S. 2016. Online monitoring of red meat color using hyperspectral imaging. *Meat Science,* 116, 110–117.

Kaswati, E. L. N., Saputro, A. H. & Imawan, C. 2020. Examination system of chicken meat quality based on hyperspectral imaging. Journal of Physics: Conference Series, 2020. IOP Publishing, 012045.

Kucha, C. T., Liu, L., Ngadi, M. & Gariépy, C. 2020. Assessment of Intramuscular Fat Quality in Pork Using Hyperspectral Imaging. *Food Engineering Reviews*, 1–16.

Leng, T., Li, F., Xiong, L., Xiong, Q., Zhu, M. & Chen, Y. 2020. Quantitative detection of binary and ternary adulteration of minced beef meat with pork and duck meat by NIR combined with chemometrics. *Food Control,* 113, 107203.

Li, Y., Shan, J., Peng, Y. & Gao, X. 2021. Nondestructive assessment of beef-marbling grade using hyperspectral imaging technology. 2011 International Conference on New Technology of Agricultural, 2011. IEEE, 779–783.

Liu, D., Pu, H., Sun, D. W., Wang, L. & Zeng, X. A. 2014. Combination of spectra and texture data of hyperspectral imaging for prediction of pH in salted meat. *Food Chemistry,* 160, 330–337.

Liu, Y., Sun, D. W., Cheng, J. H. & Han, Z. 2018. Hyperspectral imaging sensing of changes in moisture content and color of beef during microwave heating process. *Food Analytical Methods,* 11, 2472–2484.

Lohumi, S., Lee, S., Lee, H., Kim, M. S., Lee, W. H. & Cho, B. K. 2016. Application of hyperspectral imaging for characterization of intramuscular fat distribution in beef. *Infrared Physics & Technology,* 74, 1–10.

Ma, J., Sun, D. W. & Pu, H. 2017. Model improvement for predicting moisture content (MC) in pork *longissimus dorsi* muscles under diverse processing conditions by hyperspectral imaging. *Journal of Food Engineering,* 196, 65–72.

Ma, J., Sun, D. W., Pu, H., Cheng, J. H. & Wei, Q. 2019. Advanced techniques for hyperspectral imaging in the food industry: Principles and recent applications. *Annual Review of Food Science and Technology,* 10, 197–220.

Naganathan, G. K., Cluff, K., Samal, A., Calkins, C. R., Jones, D. D., Lorenzen, C. L. & Subbiah, J. 2015. Hyperspectral imaging of ribeye muscle on hanging beef carcasses for tenderness assessment. *Computers and Electronics in Agriculture,* 116, 55–64.

Naganathan, G. K., Grimes, L. M., Subbiah, J., Calkins, C. R., Samal, A. & Meyer, g. E. 2008. Visible/near-infrared hyperspectral imaging for beef tenderness prediction. *Computers and electronics in agriculture,* 64, 225–233.

Qiao, J., Ngadi, M. O., Wang, N., Gariépy, C. & Prasher, S. O. 2007. Pork quality and marbling level assessment using a hyperspectral imaging system. *Journal of Food Engineering,* 83, 10–16.

Rady, A. & Adedeji, A. A. 2020. Application of hyperspectral imaging and machine learning methods to detect and quantify adulterants in minced meats. *Food Analytical Methods,* 13, 970–981.

Rahman, S., Quin, P., Walsh, T., Vidal-Calleja, T., Mcphee, M., Toohey, E. & Alempijevic, a. 2018. Preliminary estimation of fat depth in the lamb short loin using a hyperspectral camera. *Animal Production Science,* 58, 1488–1496.

Saadatian, F., Liu, L. & Ngadi, M. 2015. Hyperspectral imaging for beef tenderness assessment. *International. Journal of Food Processing Technology,* 2, 18–25.

Tao, F. & Peng, Y. 2014. A method for nondestructive prediction of pork meat quality and safety attributes by hyperspectral imaging technique. *Journal of Food Engineering,* 126, 98–106.

Velásquez, L., Cruz-Tirado, J., Siche, R. & Quevedo, R. 2017. An application based on the decision tree to classify the marbling of beef by hyperspectral imaging. *Meat Science,* 133, 43–50.

Wu, D., Shi, H., He, Y., Yu, X. & Bao, Y. 2013. Potential of hyperspectral imaging and multivariate analysis for rapid and non-invasive detection of gelatin adulteration in prawn. *Journal of Food Engineering,* 119, 680–686.

Wu, D. & Sun, D. W. 2013a. Application of visible and near infrared hyperspectral imaging for non-invasively measuring distribution of water-holding capacity in salmon flesh. *Talanta,* 116, 266–276.

Wu, D. & Sun, D. W. 2013b. Potential of time series-hyperspectral imaging (TS-HSI) for non-invasive determination of microbial spoilage of salmon flesh. *Talanta,* 111, 39–46.

Wu, D., Sun, D. W. & He, Y. 2012. Application of long-wave near infrared hyperspectral imaging for measurement of color distribution in salmon fillet. *Innovative Food Science & Emerging Technologies,* 16, 361–372.

Yang, D., He, D., Lu, A., Ren, D. & Wang, J. 2017. Combination of spectral and textural information of hyperspectral imaging for the prediction of the moisture content and storage time of cooked beef. *Infrared Physics & Technology,* 83, 206–216.

Yang, D., Lu, A., Ren, D. & Wang, J. 2018. Detection of total viable count in spiced beef using hyperspectral imaging combined with wavelet transform and multiway partial least squares algorithm. *Journal of Food Safety,* 38, e12390.

Yang, Y., Wang, W., Zhuang, H., Yoon, S. C. & Jiang, H. 2021. Prediction of quality traits and grades of intact chicken breast fillets by hyperspectral imaging. *British Poultry Science,* 62, 46–52.

Ye, X., Iino, K. & Zhang, S. 2016. Monitoring of bacterial contamination on chicken meat surface using a novel narrowband spectral index derived from hyperspectral imagery data. *Meat Science,* 122, 25–31.

Zhang, H., Zhang, S., Chen, Y., Luo, W., Huang, Y., Tao, D., Zhan, B. & Liu, X. 2020. Non-destructive determination of fat and moisture contents in Salmon (*Salmo salar*) fillets using near-infrared hyperspectral imaging coupled with spectral and textural features. *Journal of Food Composition and Analysis,* 92, 103567.

Zhang, Y., Jiang, H. & Wang, W. 2019. Feasibility of the detection of carrageenan adulteration in chicken meat using visible/near-infrared (vis/nir) hyperspectral imaging. *Applied Sciences,* 9, 3926.

Zhao, H. T., Feng, Y. Z., Chen, W. & Jia, G. F. 2019. Application of invasive weed optimization and least square support vector machine for prediction of beef adulteration with spoiled beef based on visible near-infrared (Vis-NIR) hyperspectral imaging. *Meat Science,* 151, 75–81.

Zhao, M., Esquerre, C., Downey, G. & O'donnell, C. P. 2017. Process analytical technologies for fat and moisture determination in ground beef-a comparison of guided microwave spectroscopy and near infrared hyperspectral imaging. *Food Control,* 73, 1082–1094.

Zhao, Z., Yu, H., Zhang, S., Du, Y., Sheng, Z., Chu, Y., Zhang, D., Guo, L. & Deng, L. 2020. Visualization accuracy improvement of spectral quantitative analysis for meat adulteration using Gaussian distribution of regression coefficients in hyperspectral imaging. *Optik,* 212, 164737.

Paper received: April 3rd 2022.
Paper accepted: April 28th 2022.